Published in final edited form as:
Acc Chem Res. 2013 September 17; 46(9): 2127–2135. doi:10.1021/ar4000482.

Sensitivity and Resolution Enhanced Solid-state NMR for Paramagnetic Systems and Biomolecules under Very Fast Magic Angle Spinning

SUDHAKAR PARTHASARATHY[1,†], **YUSUKE NISHIYAMA**[3], and **YOSHITAKA ISHII**[1,2,*]

[1] Department of Chemistry, University of Illinois at Chicago, Chicago, IL, USA

[2] Center for Structural Biology, University of Illinois at Chicago, Chicago, IL, USA

[3] JEOL RESONANCE Inc., 3-1-2 Musashino, Akishimashi, Tokyo 196-8558, Japan

CONSPECTUS

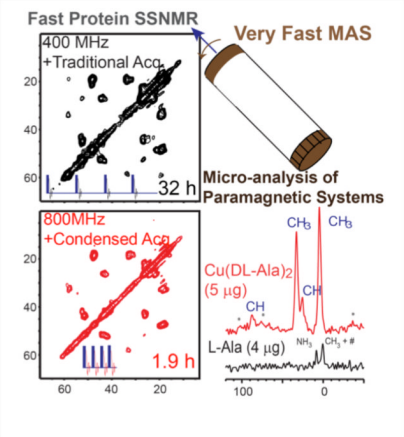

Recent research in fast magic angle spinning (MAS) methods has drastically improved in the resolution and sensitivity for NMR spectroscopy of biomolecules and materials in solids. In this Account, we summarizes recent and ongoing developments in this area by presenting ^{13}C and ^{1}H solid-state NMR (SSNMR) studies on paramagnetic systems and biomolecules under fast MAS from our laboratories.

First, we describe how very fast MAS (VFMAS) at the spinning speed of 20 kHz allows us to overcome major difficulties in ^{1}H and ^{13}C high-resolution SSNMR of paramagnetic systems. As a result, we can enhance both sensitivity and resolution by up to a few orders of magnitude. Using fast recycling (~ms/scan) using short ^{1}H T_1 values we can perform ^{1}H SSNMR micro-analysis of paramagnetic systems in the μg scale with greatly improved sensitivity over that for diamagnetic systems. Second, we discuss how VFMAS at a spinning speed greater than ~40 kHz can enhance the sensitivity and resolution of ^{13}C biomolecular SSNMR measurements. Low-power ^{1}H decoupling schemes under VFMAS offer excellent spectral resolution for ^{13}C SSNMR by nominal ^{1}H RF irradiation at ~10 kHz. By combining the VFMAS approach and enhanced ^{1}H T_1 relaxation by paramagnetic doping we can achieve extremely fast recycling in modern biomolecular SSNMR experiments. Experiments for ^{13}C-labeled ubiquitin doped with 10 mM Cu-

* To whom the corresponding should be addressed. yishii@uic.edu..
† Present address: Sigma-Aldrich, 3858 Benner Road, Miamisburg, Ohio 45342, USA

EDTA demonstrate how effectively this new approach, called *paramagnetic assisted condensed data collection* (PACC), enhances the sensitivity.

Lastly, we examine ^{13}C SSNMR measurements for biomolecules under faster MAS at a higher field. Our preliminary ^{13}C SSNMR data of Aβ amyloid fibrils and GB1 microcrystals acquired at ^{1}H NMR frequencies of 750-800 MHz suggest that the combined use of the PACC approach and the ultra-high fields could allow for routine multi-dimensional SSNMR analyses of proteins at the 50-200 nmol level. Also, we briefly discuss the prospects for studying bimolecules using ^{13}C SSNMR under ultra fast MAS at the spinning speed of ~100 kHz.

1. Introduction

SSNMR has established its status as one of the most powerful methods for non-crystalline solid materials[1,2] as well as the method of choice for structural biology.[3-5] SSNMR provides excellent structural insights for proteins in non-crystalline assemblies. Notably, for large protein assemblies such as amyloid fibrils, high-resolution SSNMR methodologies using magic angle sample spinning (MAS) have offered structural details as a *primary structural probe*.[4,6] SSNMR has also been an attractive option for structural elucidation of membrane-bound proteins and proteins in nano-/micro-crystals.[5,6] However, to date limited sensitivity and resolution have been two major bottlenecks for biomolecular SSNMR. For example, until recently, a typical multidimensional SSNMR analysis required as much as 0.5-1.0 μmol of ^{13}C-labeled samples.[3-5] For many biomolecules and advanced materials, preparing such large quantities of isotope-labeled samples is often prohibitive. The situation has been similar in SSNMR of paramagnetic materials and paramagnetic biomolecules. The magnetic nature of paramagnetic metal ions severely limits sensitivity and resolution. For this reason, in spite of the renewed importance of paramagnetic systems in modern material science, high-resolution SSNMR analysis of paramagnetic systems has been notoriously difficult. Large spectral bandwidths (500-2000 ppm) due to paramagnetic shifts make fundamental radio-frequency (RF) pulse techniques for ^{13}C and ^{1}H SSNMR, such as cross-polarization (CP) and ^{1}H RF decoupling, and ^{1}H-^{1}H dipolar decoupling, ineffective because of the difficulty in the excitation. In ^{13}C SSNMR, even under MAS, large anisotropic paramagnetic shifts (100-500 ppm) split a signal into numerous sidebands at the conventional spinning speed ($\omega_R/2\pi$ = 5-10 kHz).

In this review, we discuss recent progress in high-resolution ^{13}C and ^{1}H SSNMR of paramagnetic systems and biomolecules using fast MAS for sensitivity and resolution enhancements. We present how SSNMR for the two seemingly different research subjects of paramagnetic systems and biomolecules are interconnected by common concepts and techniques using fast MAS. Traditional SSNMR typically utilizes MAS at 5-15 kHz, which is sufficient to suppress spinning sidebands for diamagnetic spin-1/2 systems under high-power ^{1}H RF decoupling. A combination of such traditional MAS, a large amount of sample (> 50 mg), and a moderate static magnetic field (~9.4 T) has been long considered as the *optimum* scheme for SSNMR. However, recent advances in fast MAS technologies have fundamentally changed the situation, increasing achievable spinning speed to a range of 20-80 kHz.[7-12] Such fast spinning can eliminate a majority of the spin interactions in organic compounds such as ^{1}H-^{13}C and ^{1}H-^{1}H dipolar couplings as well as the large paramagnetic spin interactions, providing novel pathways of enhancing sensitivity and resolution in SSNMR. Here, we present the effectiveness of modern ^{13}C and ^{1}H SSNMR experiments with fast MAS using our recently published and new preliminary data as notable examples.

2. Resolution and Sensitivity Enhanced SSNMR of Paramagnetic Materials

More than one third of the elements in the periodic table exhibit paramagnetism. Redox reactions involving paramagnetic ions such as Cu^{2+} and Fe^{3+} often play a vital role in biological reactions and chemical catalyses.[13] High-resolution ^{13}C and ^{1}H SSNMR offers a powerful tool for structural analysis of organic materials and biomolecules. For paramagnetic systems, however, large spectral dispersion due to hyperfine shifts traditionally imposed severe technical difficulties in high-resolution ^{13}C and ^{1}H SSNMR studies, prohibiting applications of essential SSNMR techniques such as ^{1}H decoupling, MAS, and CP. SSNMR of $^{7}Li/^{6}Li$ and other abundant spins has been effective for analysis of paramagnetic inorganic systems,[14] yet these options are not available for a variety of paramagnetic complexes. Although there were a handful of excellent studies that involve selective ^{2}D- or ^{13}C-labeling,[15,16] in general, applications of SSNMR to paramagnetic systems have been severely hampered.

2.1. ^{1}H SSNMR of Paramagnetic Systems by Very Fast MAS

Recently, our group has reestablished ^{1}H and ^{13}C SSNMR as a method applicable to a broad array of paramagnetic complexes using very-fast MAS (VFMAS) at the spinning speed of 20 kHz or more, which we call *VFMAS approach*.[17-21] As the spinning speed in the approach becomes comparable to the magnitude of major spin interactions in organic solids such as ^{1}H-^{13}C and ^{1}H-^{1}H dipolar couplings, the VFMAS approach effectively removes homogeneous line broadening due to these interactions. Figure 1a-c shows the spinning speed dependence of ^{1}H MAS spectra of $Cu(DL\text{-}Ala)_2\bullet(H_2O)$. Clearly, a high-resolution ^{1}H SSNMR spectrum is observed in (a) at the spinning speed of 24 kHz, which sufficiently suppresses large anisotropic paramagnetic shifts spanning ~200 ppm as well as ^{1}H-^{1}H dipolar couplings. Only 18 ms of the experimental time was required for collecting the high-quality spectrum with 4 scans for 17 mg of the sample because of the fast recycling (~5 ms) offered by very short paramagnetic ^{1}H T_1 relaxation time (~1.5 ms). In contrast, very weak or nearly no signals are observed at the spinning speed of 5-10 kHz in (b, c) because of splitting into numerous sidebands and line broadening due to paramagnetic interactions. It is noteworthy that large anisotropic paramagnetic shifts originate from the thermally averaged dipolar interactions between paramagnetic electron spin and nuclear spin.[20,22] The anisotropic paramagnetic shifts are generally proportional to $(S+1)S\gamma_I/R_{IS}^3$,[22] where γ_I is the gyromagnetic ratio of the nuclear spin *I*, *S* is an electron spin number, and R_{IS} is the distance between *I* and the electron spin *S* at the paramagnetic center ($S=1/2$ for Cu^{2+}). Thus, for a paramagnetic metal ion having a larger electronic spin number *S*, the range of the paramagnetic shift can be even greater. The VFMAS approach is effective for such systems having larger paramagnetic shifts. Figure 1d-f shows the spinning-speed dependence of ^{1}H MAS spectra of $Mn(acac)_3$ (S = 5/2; 14 mg). Clearly, well resolved ^{1}H lines are observed for CH_3 and CH group for $Mn(acac)_3$ in (d). The system has extremely large paramagnetic shifts spanning ~800 ppm (or 320 kHz). For these types of systems, traditional high-resolution ^{1}H SSNMR techniques such as CRAMPS[23] are not effective. In contrast, VFMAS approach, which utilizes averaging by sample spinning, is effective, regardless of large resonance offsets due to paramagnetic shifts. These data prove that the VFMAS approach enhances sensitivity and resolution by a few orders of magnitude, greatly impacting SSNMR analysis of paramagnetic systems.[17,19,21]

2.2. ^{1}H SSNMR for Microanalysis of Paramagnetic Systems under VFMAS

The short T_1 values of paramagnetic systems are highly beneficial for enhancing the sensitivity of SSNMR in the VFMAS approach. Figure 2 displays an example of ^{1}H SSNMR micro analysis by comparing a ^{1}H SSNMR spectrum of (a) $Cu(L\text{-}Ala)_2$ (20 nmol or 5.0 μg) with that of a diamagnetic control (b) L-Ala (40 nmol or 4.0 μg). For the most intense CH_3 signal, the signal-to-noise ratio (S/N) of 41 was obtained within 2 min for (a).

Hence, analyzing several nmol of the paramagnetic samples is feasible by SSNMR. With improved resolution under VFMAS, the spectrum for $Cu(L\text{-}Ala)_2$ in (a) shows distinctive spectral features from those of $Cu(DL\text{-}Ala)_2$ (**Fig. 1a**). In a control experiment for 40 nmol (3.8 μg) of L-Ala shown in Fig. 2b, we obtained a S/N of 3.4 for the peak at 8.2 ppm, which corresponds to NH_3^+, in a common experimental time (2 min). Note that the slightly greater CH_3 signal at ~1 ppm overlaps with a background signal (marked by #). Therefore, the results support an intriguing conclusion that with the aid of the VFMAS approach, SSNMR of paramagnetic systems yields about a 10-fold sensitivity advantage over SSNMR of the diamagnetic system for unit sample amount (i.e. 40 nmol of Ala). Although we will not discuss the details, our group and other demonstrated that the VFMAS approach is also highly effective for ^{13}C SSNMR for a variety of paramagnetic systems.[18,20,21,24] Traditional CPMAS approaches are not effective for paramagnetic systems because of large spectral dispersions and anisotropic hyperfine shifts. Strong RF fields available at the VFMAS probes offer sensitivity-enhanced ^{13}C SSNMR for paramagnetic systems via polarization transfer from ^1H by dipolar INEPT or CP,[18,19] combined with the advantage of short ^1H T_1 values due to paramagnetic relaxation. As will be described below, we demonstrate that a similar sensitivity-enhancement approach using paramagnetic relaxation enhancements is feasible for non-paramagnetic systems, including proteins, under VFMAS.

3. New Opportunities in Studying Biomolecules by VFMAS

3.1. Low-power decoupling under VFMAS

VFMAS approach also opens an avenue to novel SSNMR methodologies for non-paramagnetic systems. Since the spinning speed is comparable to or greater than strongest spin interactions in organic solids, such as ^{13}C-^1H and ^{15}N-^1H dipolar couplings, non-traditional strategies of SSNMR experiments can produce optimum results. One area of great interest is ^1H decoupling since traditional decoupling for SSNMR requires high power irradiation of ^1H RF fields, which may result in the degradation of heat sensitive biological samples or probe arcing. Ishii and Tycko showed the effectiveness of cw low-power ^1H decoupling for ^1H detected 2D ^{13}C and ^{15}N SSNMR experiments under VFMAS at 30 kHz.[8,25] Recently, Ernst *et al.* examined the low-power decoupling using cw and XiX decoupling sequences, the latter of which offers excellent resolution.[9,26] Here, we show examples of applications using an alternative low-power TPPM decoupling sequence, which provides a slightly better performance over low-power XiX.[10]

Figure 3 shows the ^1H decoupling dependence of ^{13}C CPMAS spectra of uniformly ^{13}C- and ^{15}N-labeled L-ala under VFMAS at 40 kHz that were obtained with (a) low-power TPPM (lpTPPM) decoupling at the RF field ($\omega_1/2\pi$) of 10 kHz, (b) cw decoupling at $\omega_1/2\pi$ of 200 kHz, and (c) TPPM decoupling at $\omega_1/2\pi$ of 200 kHz. Under VFMAS, the lpTPPM ^1H decoupling in (a) yielded superior resolution and sensitivity over the cw decoupling at 200 kHz in (b). Considering that the lpTPPM sequence requires only 0.25 % of the RF power used for the sequences in (b, c), it is striking that lpTPPM offers comparable performance to that of the high-power TPPM in (c). With this low-power sequence, the recycle delay can be adjusted to the optimum value with nearly no restrictions due to sample heating problems.[10,27] Probe arcing is rarely the issues with lpTPPM. With these advantages, low-power ^1H decoupling sequences such as lpTPPM,[10] XiX,[9] and recent variants[28] are replacing high-power decoupling under VFMAS at 40-50 kHz or above in many recent biological applications, where sample degradation by rf irradiation should be avoided.[29-33] Reflecting major changes in the SSNMR methodologies, MAS at a spinning speed above 40-50 kHz is often called *ultra-fast MAS* in recent articles.[31,34-36] As will be discussed in the next section, the low-power decoupling offers a key tool in sensitivity enhancements with extremely fast recycling.

3.2. Sensitivity enhancement by PACC by use of Paramagnetic Relaxation Enhancement

Restricted sensitivity of SSNMR is one of the major bottlenecks in SSNMR-based structural analysis. Typically, as much as 0.5-1 μmol of an isotope labeled sample is required for basic multidimensional SSNMR experiments, which severely limits biological applications. Since the introduction of high-resolution ^{13}C SSNMR by the CPMAS method, data collection for SSNMR has been inefficient due to long idling delays required for magnetization recovery through ^{1}H T_1 relaxation between scans. Even in modern multi-dimensional SSNMR schemes, 95-99 % of the experimental time is typically “wasted” for recycle delays.

Recently, we proposed an approach to break the long-standing ^{1}H T_1 boundary problem for hydrated proteins by combining paramagnetic doping, very-fast magic-angle spinning (MAS), and fast recycling of the low-rf-power sequences.[21,25] In this approach, which we call “paramagnetic-relaxation-assisted condensed data collection” (PACC), we achieve a reduction in ^{1}H T_1 by orders of magnitude down to 50-100 ms by carefully adjusting the paramagnetic-doping level.[11,27,37] Figure 4(a, b) shows a comparison of 1D ^{13}C CPMAS spectra of (a) ^{13}C- and ^{15}N-labeled ubiquitin microcrystals doped with 10 mM Cu^{2+}-EDTA and (b) undoped ubiquitin microcrystals. The spectrum in (a) was collected with the PACC approach with a recycle delay of 150 ms while that in (b) was collected by a conventional CPMAS method with a recycle delay of 0.7 s. With the PACC approach, the data collection was effectively accelerated by ~5 fold in (a). The difference spectrum in (c) clearly shows only negligible changes in the ^{13}C spectrum due to the fast recycling or the addition of Cu-EDTA. Cu-EDTA was selected as dopants since Cu^{2+} ions with an optimum electron-spin correlation time (τ_e~10^{-9} s) reduces T_1 considerably without substantial paramagnetic broadening in $^{13}C/^{15}N$ SSNMR spectra unlike Gd^{3+} ions and nitroxide radicals, which introduce severer broadening for their longer τ_e (10^{-8}-10^{-7} s).[11] To attain extreme fast recycling with the recycle delay matched to $3T_1$, we employed the lpTPPM ^{1}H decoupling at $\omega_1/2\pi$ of 10 kHz in both (a, b) under VFMAS at 40 kHz. As the acquisition periods of (a, b) are ~30 ms, recycle delays of 2-3 s would be needed with traditional high-power ^{1}H decoupling in order to avoid sample heating or probe arcing; the required delays are often much longer than typical ^{1}H T_1 of hydrated proteins (300-500 ms). Overall, compared with the traditional CPMAS using high-power decoupling, the PACC approach provides acceleration of data collection by a factor of up to 20.

Figure 4d shows a comparison of 2D $^{13}C/^{13}C$ correlation spectra of (red) uniformly ^{13}C- and ^{15}N-labeled ubiquitin with Cu-EDTA collected by the PACC approach and (black) undoped ubiquitin by a standard experiment. Although a moderate static magnetic field of 9.4 T (^{1}H NMR frequency of 400.2 MHz) was used, a 2D spectrum of excellent quality (**Fig. 4d** red) was collected only in 5.4 h with the PACC approach for 1.8 mg (~200 nmol) of ubiquitin, while the traditional experiment without the PACC approach required 21.9 h to obtain a similar 2D spectrum (**Fig. 4d** black). The superimposed 2D spectra (**Fig. 4d**) and the 1D slices (**Fig. 4e**) show both the doped and undoped samples yielded almost identical spectra. Despite the relatively short intrinsic ^{1}H T_1 values of the undoped samples, the experimental time was still reduced by 4 folds. We also demonstrated that the PACC approach allows us to collect a 2D $^{13}C/^{15}N$ correlation SSNMR spectrum with as little as 22 nmol (~200 μg) of ubiquitin within 2.7 h at the ^{1}H NMR frequency of 400 MHz. The PACC approach and its variations are now widely used for a wide variety of systems including amyloid fibrils,[11,38] membrane proteins,[30,39] highly deuterated proteins,[37] and metal-bound proteins.[29,38] Recent studies showed that proteins modified with adequate Cu^{2+}-chelator tags offer long-range distance information with condensed data collection by the PACC method.[40,41] Additional examples of structural measurements using paramagnetic interactions are available in other references[11,42,43] and an excellent review by Jaroniec et al.[44]

4. Motivation and Prospects of Studying Biomolecules by Faster MAS in a Higher Field

4.1. SSNMR applications in an ultra-high-field using VFMAS

The VFMAS approach and the PACC approach are potentially effective for SSNMR spectroscopy in an ultra-high magnetic field. So far, only a few such examples were recently presented.[29,30] Using the PACC scheme at an ultra-high field at the ^{1}H NMR frequency of 750 MHz (17.6 T), we have obtained preliminary (a) 2D ^{13}C/^{13}C correlation spectrum and (b) overlaid 3D NCACO (blue) and CANCO (red) spectra on uniformly ^{13}C- and ^{15}N-labeled GB1 microcrystals (~2 mg or 300 nmol) doped with 30 mM Cu(II)-EDTA at MAS of 60 kHz using a new 750 MHz SSNMR system at UIC with the PACC approach (**Fig. 5**). Figure 5 shows excellent resolution in the 2D and 3D spectra that were respectively collected in only 15 min and 1 h each. Our data at 750 MHz in Fig. 5 clearly demonstrate the possibility of completing sequential assignments after several hours for a few mg of the protein. Taken as a whole, the data demonstrate distinctive sensitivity and resolution advantage of ultra-high field SSNMR under VFMAS using the PACC approach over a traditional SSNMR approach in a lower field.

The PACC approach in an ultra-high field is also effective for heterogeneous protein samples such as amyloid fibrils. Here, we compare 2D ^{13}C/^{13}C correlation SSNMR spectra of Cu^{2+}-bound Aβ(1-40) fibrils[38] (**Fig. 6a, b**) collected at ^{1}H NMR frequencies of (a) 400 MHz and (b) 800 MHz. The data were obtained with mixing by the fpRFDR scheme[45] (a) at $\omega_R/2\pi$ of 20 kHz with high-power ^{1}H decoupling at 90 kHz and (b) under fast MAS at $\omega_R/2\pi$ of 50 kHz with low-power ^{1}H decoupling at 12.5 kHz. In (b), using the PACC approach with short recycle delays (~270 ms), we could collect a nicely resolved spectrum in 1.9 h with a slightly better signal-to-noise ratio (S/N) for only 1 mg of the Aβ sample, compared with that for (a), which required 32 h of signal accumulation for 2 mg of the same sample. In (a), the recycle delay (~1.8 s) was restricted by probe arcing under high-power ^{1}H decoupling (8 ms). For a unit amount of the sample, this is equivalent to 60-fold acceleration of the experiment by effective use of the PACC approach and ultra-high field SSNMR. As the 1 mm JEOL CPMAS probe used for this study offers spinning up to 80 kHz,[12] further sensitivity/resolution enhancements are possible in combination with ^{1}H detected SSNMR.[8,25,34] The development of such experimental schemes is ongoing in our laboratory.

4.2. Faster MAS at ~100 kHz and prospects of its applications of biomolecules

Recent engineering efforts to develop fast MAS technologies have achieved sample spinning at $\omega_R/2\pi$ of ~100 kHz or higher. Such fast MAS methods are likely to offer opportunities for novel NMR approaches as the spinning speed now approaches 2-4 folds of major spin interactions in organic solids such as ^{1}H-^{1}H and ^{1}H-^{13}C dipolar couplings. On the other hand, under MAS over ~100 kHz, traditionally useful RF schemes may no longer be effective especially for biomolecules, for which applicable RF fields are restricted due to sample heating. For example, for efficient CP under fast MAS, the ^{1}H RF field (ω_H) is typically matched at $\omega_H = <\omega_C> + \omega_R$, where $<\omega_C>$ is the average ^{13}C RF field for the ramped CP sequence, and the ω_H value is ~2.5ω_R. However, for MAS at 100 kHz, such RF values of ω_H and ω_C become prohibitively large for heat-labile biomolecule samples (i.e. $\omega_H/2\pi$~ 250 kHz). To address this problem, we have explored a low-power CP (lpCP) scheme, such as double-quantum ^{1}H-^{13}C CP (DQ-CP), which was previously introduced by our group for ^{15}N-^{13}C CP at $\omega_R/2\pi$ of 40 kHz.[11] Although ^{1}H-^{13}C lpCP schemes were successfully employed under VFMAS at 40-60 kHz,[34,46] our experiments showed that the CP efficiencies of such lpCP are generally lower than those for high-power CP at spinning speeds of 40-70 kHz. In our preliminary data using a proto-type JEOL 0.75-mm MAS probe

at $\omega_R/2\pi$ of 98 kHz (^{1}H NMR frequency of 600 MHz), we compared the ^{13}C CPMAS spectra of uniformly ^{13}C- and ^{15}N-labeled L-alanine (U ^{13}C, and ^{15}N L-Ala; **Fig. 7**) obtained with (a) DQ-CP ($\omega_H/2\pi$ ~74 kHz, $\omega_C/2\pi$ ~24 kHz) and (b) standard CP with (c) a ^{13}C MAS spectrum with $\pi/2$-pulse excitation. To our surprise, we have found that the low-power DQ-CP sequence provides better CP efficiencies (red factors in **Fig. 7**) for CO_2 and CH_3 than those for the standard CP as shown in (a) and (b). This is most likely attributed to a combination of higher spin lock efficiency under faster MAS[32] and smaller CP mismatching due to RF-inhonogeneity by the use of weaker RF fields in lpCP.[46] It is also noteworthy that the enhancement factors observed here are comparable to or higher than the corresponding values obtained at a much lower spinning speed of ~20 kHz. This clearly indicates new opportunities for designing more efficient low-power CP schemes using MAS over 100 kHz, contrary to a common conception that CP efficiencies become lower at a faster MAS rate. The notable resolution (**Fig. 7d-f**) was obtained by low-power TPPM at $\omega_H/2\pi$ ~10 kHz. As the sensitivity and resolution form a critical foundation of biomolecular SSNMR, the data provide excellent prospects for future use of extremely fast MAS for biomolecular SSNMR.

Acknowledgments

The development of novel SSNMR approaches was supported primarily by the NSF (CHE 0449952, CHE 957793). Structural studies of the amyloid fibrils were supported mainly by the NIH (9R01 GM098033) and in part by the Alzheimer's Association (IIRG; 08-91256) and Dreyfus Foundation Teacher-Scholar Award. The instrumentation of the 750 MHz SSNMR was supported by the NIH (1S10 RR025105). We thank the JEOL Resonance for making the prototype 1-mm and 0.75-mm MAS probes available for this study. In particular, we thank Drs. Yuki Endo and Takahiro Nemoto at the JEOL Resonance for their excellent design works. We are grateful to Dr. Jochem Struppe for his advice on pulse sequences on the Bruker Avance spectrometers and Dr. Kazuo Yamauchi at the King Abdullah University of Science and Technology for prompting us to be involved in the 1mm probe project. We also thank Dr. Fei Long and Mr. Isamu Matsuda for providing the GB1 sample and Dr. William Tay for useful comments about this manuscript. YI is grateful to the late Prof. Ivano Bertini for his encouragements in the course of our studies on paramagnetic SSNMR of materials and biomolecules.

Biography

Sudhakar Parthasarathy is an analytical scientist at Sigma-Aldrich Corporation. He received his B.S, M.S at University of Madras, India and his Ph.D. at the University of Illinois at Chicago with Prof. Ishii. He has studied paramagnetic biomolecules by SSNMR.

Yusuke Nishiyama is a research scientist at JEOL RESONANCE Inc. He received his B.A. and Ph.D. at Kyoto University, Japan. In 2007, he joined JEOL Inc, the NMR division of which recently span off as JEOL RESONANCE Inc. He develops exotic NMR methodologies for materials and biological applications.

Yoshitaka Ishii is a Professor of Chemistry at the University of Illinois at Chicago, where he has been faculty since 2001. He received his B.A. and Ph.D. at Kyoto University. Prof. Ishii aims to develop innovative SSNMR methodologies and seeks novel applications of the developed methods to biological systems and materials.

References

1. Schmidt-Rohr, K.; Spiess, HW. Multidimensional solid-state NMR and polymers. Academic Press Inc.; San Diego: 1994.
2. Grey CP, Goward GR. Special Issue: Solid-State NMR in Materials for Energy Storage and Conversion. Solid State Nucl. Magn. Reson. 2012; 42:1–1. [PubMed: 22445132]
3. Baldus M. Molecular interactions investigated by multi-dimensional solid-state NMR. Curr. Opin. Struct. Biol. 2006; 16:618–623. [PubMed: 16942870]

4. Tycko R. Molecular structure of amyloid fibrils: insights from solid-state NMR. Q. Rev. Biophys. 2006; 39:1–55. [PubMed: 16772049]

5. McDermott A. Structure and Dynamics of Membrane Proteins by Magic Angle Spinning Solid-State NMR. Annual Review of Biophysics. 2009; 38:385–403.

6. Baldus M. Solid-state NMR spectroscopy: Molecular structure and organization at the atomic level. Angew. Chem. Int. Edit. 2006; 45:1186–1188.

7. Schnell I, Spiess HW. High-resolution H-1 NMR spectroscopy in the solid state: Very fast sample rotation and multiple-quantum coherences. J. Magn. Reson. 2001; 151:153–227. [PubMed: 11531343]

8. Ishii Y, Tycko R. Sensitivity enhancement in solid state 15N NMR by indirect detection with high-speed magic angle spinning. J. Magn. Reson. 2000; 142:199–204. [PubMed: 10617453]

9. Ernst M, Samoson A, Meier BH. Low-power XiX decoupling in MAS NMR experiments. J. Magn. Reson. 2003; 163:332–339. [PubMed: 12914849]

10. Kotecha M, Wickramasinghe NP, Ishii Y. Efficient low-power heteronuclear decoupling in 13C high-resolution solid-state NMR under fast magic angle spinning. Magn. Reson. Chem. 2007; 45:S221–230. [PubMed: 18157841]

11. Wickramasinghe NP, Parthasarathy S, Jones CR, Bhardwaj C, Long F, Kotecha M, Mehboob S, Fung LWM, Past J, Samoson A, Ishii Y. Nanomole-scale protein solid-state NMR by breaking intrinsic H-1 T-1 boundaries. Nature Methods. 2009; 6:215–218. [PubMed: 19198596]

12. Nishiyama Y, Endo Y, Nemoto T, Utsumi H, Yamauchi K, Hioka K, Asakura T. Very fast magic angle spinning H-1-N-14 2D solid-state NMR: Sub-micro-liter sample data collection in a few minutes. J. Magn. Reson. 2011; 208:44–48. [PubMed: 21035366]

13. Bertini, I.; Gray, HB.; Lippard, SJ.; Valentine, JS. Bioinorganic Chemistry. University Science Books; Sausalito, CA: 1994.

14. Zhang Y, Sun HH, Oldfield E. Solid-state NMR Fermi contact and dipolar shifts in organometallic complexes and metalloporphyrins. J. Am. Chem. Soc. 2005; 127:3652–3653. [PubMed: 15771472]

15. Brough AR, Grey CP, Dobson CM. Paramagnetic ions as structural probes in solid-state NMR: distance measurements in crystalline lanthanide acetates. J. Am. Chem. Soc. 1993; 115:7318–7327.

16. Liu K, Ryan D, Nakanishi K, McDermott A. Solid-State NMR-Studies of Paramagnetic Coordination-Complexes - a Comparison of Protons and Deuterons in Detection and Decoupling. J. Am. Chem. Soc. 1995; 117:6897–6906.

17. Wickramasinghe NP, Shaibat M, Ishii Y. Enhanced sensitivity and resolution in 1H solid-state NMR spectroscopy of paramagnetic complexes under very fast magic angle spinning. J. Am. Chem. Soc. 2005; 127:5796–5797. [PubMed: 15839671]

18. Ishii Y, Chimon S, Wickramasinghe NP. A new approach in 1D and 2D 13C high resolution solid-state NMR spectroscopy of paramagnetic organometallic complexes by very fast magic-angle spinning. J. Am. Chem. Soc. 2003; 125:3438–3439. [PubMed: 12643699]

19. Wickramasinghe NP, Ishii Y. Sensitivity enhancement, assignment, and distance measurement in 13C solid-state NMR spectroscopy for paramagnetic systems under fast magic angle spinning. J. Magn. Reson. 2006; 181:233–243. [PubMed: 16750405]

20. Wickramasinghe NP, Shaibat M, Ishii Y. Elucidating connectivity and metal binding structures in unlabeled paramagnetic systems by 13C high-resolution solid-state NMR spectroscopy under fast magic angle spinning. J. Phys. Chem. B. 2007; 111:9693–9696. [PubMed: 17661508]

21. Wickramasinghe NP, Shaibat M, Casabianca LB, de Dios AC, Harwood JS, Ishii Y. Progress in 13C and 1H solid-state NMR for paramagnetic systems under very fast MAS. J. Chem. Phys. 2008; 128:52210.

22. Bertini, I.; Luchinat, C.; Parigi, G. Solution NMR of paramagnetic molecules. Elsevier Science B. V.; Amsterdam, The Netherlands: 2001.

23. Ernst, RR.; Bodenhausen, G.; Wokaun, A. Principles of nuclear magnetic resonance in one and two dimensions. 1st ed.. Oxford University Press; Oxford: 1987.

24. Kervern G, Pintacuda G, Zhang Y, Oldfield E, Roukoss C, Kuntz E, Herdtweck E, Basset JM, Cadars S, Lesage A, Coperet C, Emsley L. Solid-state NMR of a paramagnetic DIAD-Fe-II

catalyst: Sensitivity, resolution enhancement, and structure-based assignments. J. Am. Chem. Soc. 2006; 128:13545–13552. [PubMed: 17031968]

25. Ishii Y, Yesinowski JP, Tycko R. Sensitivity enhancement in solid-state C-13 NMR of synthetic polymers and biopolymers by H-1 NMR detection with high-speed magic angle spinning. J. Am. Chem. Soc. 2001; 123:2921–2922. [PubMed: 11456995]
26. Ernst M, Samoson A, Meier BH. Low-power decoupling in fast magic-angle spinning NMR. Chem. Phys. Lett. 2001; 348:293–302.
27. Wickramasinghe NP, Kotecha M, Samoson A, Past J, Ishii Y. Sensitivity enhancement in 13C solid-state NMR of protein microcrystals by use of paramagnetic metal Ions for optimizing 1H T1 relaxation. J. Magn. Reson. 2007; 184:350–356. [PubMed: 17126048]
28. Mithu VS, Paul S, Kurur ND, Madhu PK. Heteronuclear dipolar decoupling in solid-state nuclear magnetic resonance under ultra-high magic-angle spinning. J. Magn. Reson. 2011; 209:359–363. [PubMed: 21354839]
29. Knight MJ, Pell AJ, Bertini I, Felli IC, Gonnelli L, Pierattelli R, Herrmann T, Emsley L, Pintacuda G. Structure and backbone dynamics of a microcrystalline metalloprotein by solid-state NMR. Proc. Natl. Acad. Sci. U. S. A. 2012; 109:11095–11100. [PubMed: 22723345]
30. Tang M, Berthold DA, Rienstra CM. Solid-State NMR of a Large Membrane Protein by Paramagnetic Relaxation Enhancement. Journal of Physical Chemistry Letters. 2011; 2:1836–1841. [PubMed: 21841965]
31. Bertini I, Emsley L, Felli IC, Laage S, Lesage A, Lewandowski JR, Marchetti A, Pierattelli R, Pintacuda G. High-resolution and sensitivity through-bond correlations in ultra-fast magic angle spinning (MAS) solid-state NMR. Chemical Science. 2011; 2:345–348.
32. Lewandowski JR, Sass HJ, Grzesiek S, Blackledge M, Emsley L. Site-Specific Measurement of Slow Motions in Proteins. J. Am. Chem. Soc. 2011; 133:16762–16765. [PubMed: 21923156]
33. Vijayan V, Demers JP, Biernat J, Mandelkow E, Becker S, Lange A. Low-power solid-state NMR experiments for resonance assignment under fast magic-angle spinning. Chemphyschem : a European journal of chemical physics and physical chemistry. 2009; 10:2205–8. [PubMed: 19603450]
34. Marchetti A, Jehle S, Felletti M, Knight MJ, Wang Y, Xu Z-Q, Park AY, Otting G, Lesage A, Emsley L, Dixon NE, Pintacuda G. Backbone Assignment of Fully Protonated Solid Proteins by 1H Detection and Ultrafast Magic-Angle-Spinning NMR Spectroscopy. Angew. Chem. Int. Edit. 2012; 51:10756–10759.
35. Laage S, Sachleben JR, Steuernagel S, Pierattelli R, Pintacuda G, Emsley L. Fast acquisition of multi-dimensional spectra in solid-state NMR enabled by ultra-fast MAS. J. Magn. Reson. 2009; 196:133–141. [PubMed: 19028122]
36. Bertini I, Emsley L, Lelli M, Luchinat C, Mao J, Pintacuda G. Ultrafast MAS Solid-State NMR Permits Extensive C-13 and H-1 Detection in Paramagnetic Metalloproteins. J. Am. Chem. Soc. 2010; 132:5558–+. [PubMed: 20356036]
37. Linser R, Chevelkov V, Diehl A, Reif B. Sensitivity enhancement using paramagnetic relaxation in MAS solid-state NMR of perdeuterated proteins. J. Magn. Reson. 2007; 189:209–216. [PubMed: 17923428]
38. Parthasarathy S, Long F, Miller Y, Xiao Y, Thurber K, McElheny D, B. M, Nussinov R, Ishii Y. Molecular-level examination of Cu2+ binding structure for amyloid fibrils of 40-residue Alzheimer's beta by solid-state NMR spectroscopy. J. Am. Chem. Soc. 2011; 133:3390–3400. [PubMed: 21341665]
39. Yamamoto K, Xu J, Kawulka KE, Vederas JC, Ramamoorthy A. Use of a Copper-Chelated Lipid Speeds Up NMR Measurements from Membrane Proteins. J. Am. Chem. Soc. 2010; 132:6929–+. [PubMed: 20433169]
40. Nadaud PS, Helmus JJ, Sengupta I, Jaroniec CP. Rapid Acquisition of Multidimensional Solid-State NMR Spectra of Proteins Facilitated by Covalently Bound Paramagnetic Tags. J. Am. Chem. Soc. 2010; 132:9561–9563. [PubMed: 20583834]
41. Sengupta I, Nadaud PS, Helmus JJ, Schwieters CD, Jaroniec CP. Protein fold determined by paramagnetic magic-angle spinning solid-state NMR spectroscopy. Nature Chemistry. 2012; 4:410–417.

42. Balayssac S, Bertini I, Bhaumik A, Lelli M, Luchinat C. Paramagnetic shifts in solid-state NMR of proteins to elicit structural information. Proc. Natl. Acad. Sci. U. S. A. 2008; 105:17284–17289. [PubMed: 18988744]

43. Bertini I, Bhaumik A, De Paepe G, Griffin RG, Lelli M, Lewandowski JR, Luchinat C. High-Resolution Solid-State NMR Structure of a 17.6 kDa Protein. J. Am. Chem. Soc. 2010; 132:1032–1040. [PubMed: 20041641]

44. Jaroniec CP. Solid-state nuclear magnetic resonance structural studies of proteins using paramagnetic probes. Solid State Nucl. Magn. Reson. 2012; 43-44:1–13. [PubMed: 22464402]

45. Ishii Y. 13C-13C dipolar recoupling under very fast magic angle spinning in solid-state NMR: Applications to distance measurements, spectral assignments, and high-throughput secondary-structure elucidation. J. Chem. Phys. 2001; 114:8473–8483.

46. Lange A, Scholz I, Manolikas T, Ernst M, Meier BH. Low-power cross polarization in fast magic-angle spinning NMR experiments. Chem. Phys. Lett. 2009; 468:100–105.

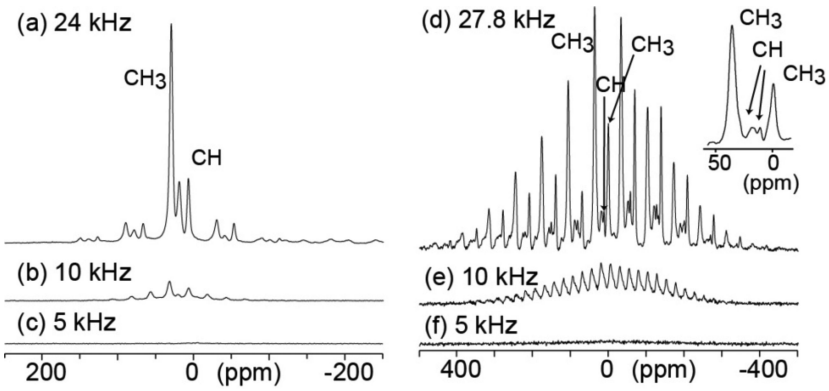

Figure 1.

Spinning speed dependence of ^{1}H MAS spectra of (a-c) $Cu(DL\text{-}Ala)_2 \cdot (H_2O)$ and (d-f) $Mn(acac)_3$ obtained at ^{1}H NMR frequency of 400.2 MHz by $\pi/2$-pulse excitation. The spinning speed is indicated in the figure. The inset in (d) is the expanded center line region. The spectra were obtained at ^{1}H frequency of 400.2 MHz with 1-pulse excitation and a rotor synchronous echo with 4 scans for each spectrum. The assignment for $Cu(DL\text{-}Ala)_2$ and $Mn(acac)_3$ was obtained from separate 2D $^{13}C/^{1}H$ correlation NMR experiments. The total experimental times were only (a-c) 18 ms and (d-f) 12 ms. The data were modified from ref. 17.

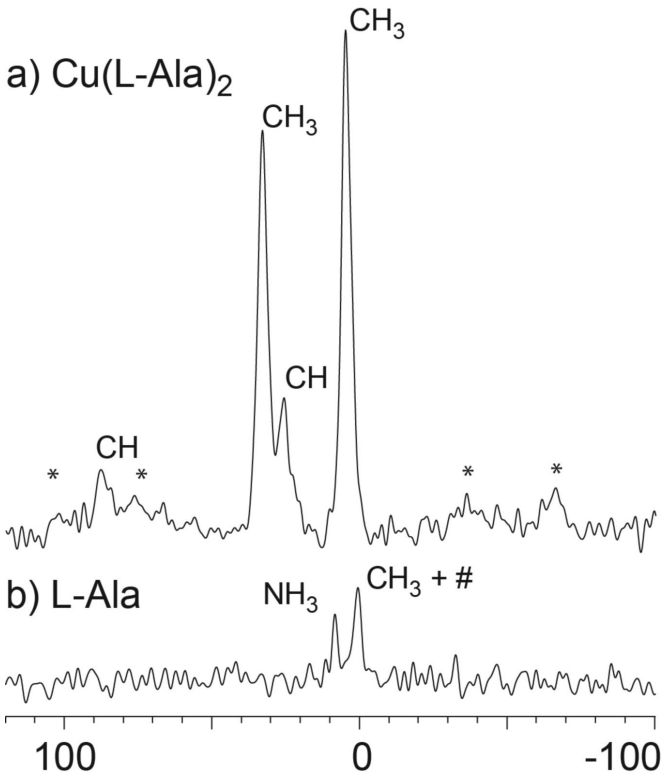

Figure 2.

^{1}H VFMAS spectra of (a) Cu(L-Ala)$_2$ and (b) L-Ala obtained at the ^{1}H NMR frequency of 400.2 MHz with one-pulse excitation at the spinning speed of 28.57 kHz. The sample amounts are (a) 20 nmoles (5 μg) and (b) 40 nmoles (4 μg). An experimental time was 2 min each. A total of (a) 38,700 and (b) 76 scans were recorded with recycle delays of (a) 3 ms and (b) 1.6 s, respectively. Background signals and spinning sidebands are marked by # and *, respectively. The spectrum (a) is scaled so that the two spectra display a common noise level. The data were modified from ref. 17.

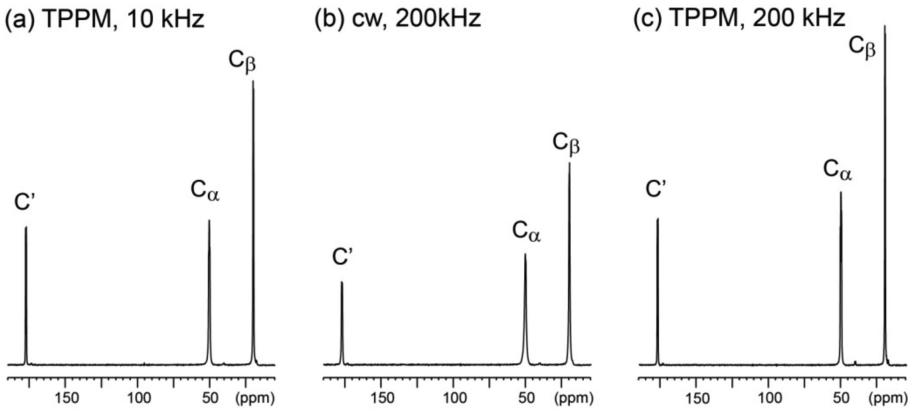

Figure 3.

^{13}C CPMAS spectra of L-alanine obtained at the ^{13}C NMR frequency of 100.6 MHz (9.4 T) by the (a) low-power TPPM (lpTPPM), (b) high-power cw and (c) high-power TPPM ^{1}H decoupling sequences at the spinning speed of 40 kHz. The rf-field intensities used for the low-power and high-power decoupling sequences are 10 kHz and 200 kHz, respectively. In the lpTPPM sequence, the pulse width (τ_W) was 49 μs and the phase was alternated between $-\varphi$ and φ ($\varphi = 18.5°$), while for high-power TPPM τ_W was 2.54 μs and $\varphi = 10.5°$. The pulse width and the phase angle were carefully optimized. The spectra are scaled by a common scale for comparison. The data were modified from ref. 10.

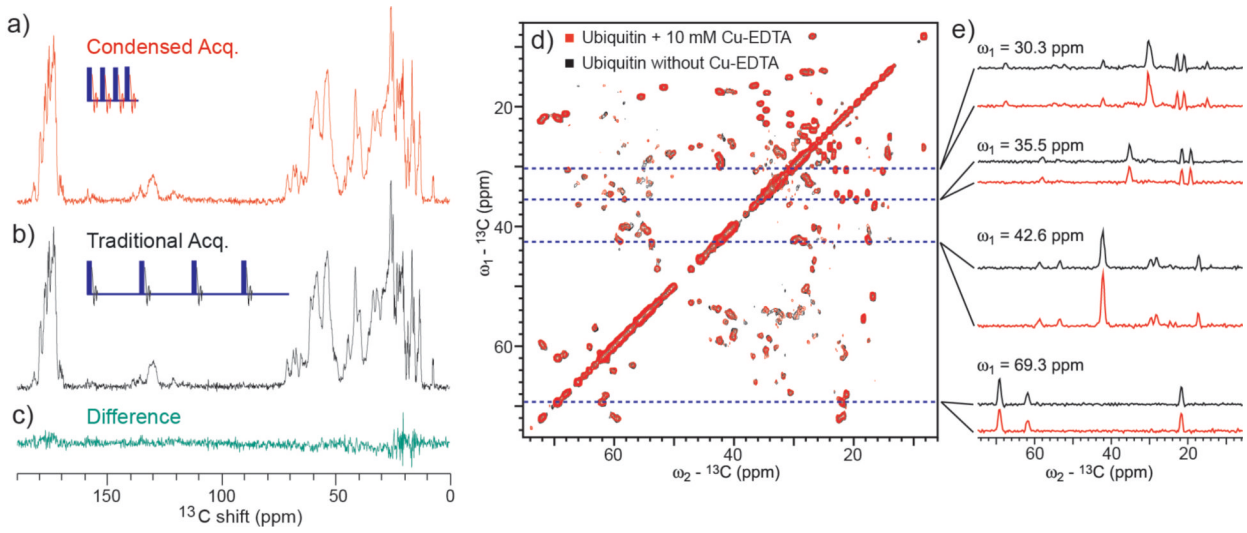

Figure 4.

Comparison of (a-c) 1D ^{13}C CPMAS spectra and (d) superimposed 2D $^{13}C/^{13}C$ chemical-shift correlation solid-state NMR spectra of microcrystalline uniformly ^{13}C-labeled ubiquitin in microcrystals (1.8 mg) in the (red) presence and (black) absence and of 10 mM Cu(II)-EDTA at the ^{1}H frequency of 400.2 MHz. In (red) PACC approach and (black) traditional signal collection for (a-c), the recycle delays of 150 ms and 700 ms were set to 3 times the T_1 values, respectively. The green spectrum (c) is the difference of (a) and (b). In (a, b), signals of 256 scans were accumulated with the total experimental times of (red) 0.7 min and (black) 3.1 min. (d) Comparison of superimposed 2D $^{13}C/^{13}C$ correlation SSNMR spectra of the ^{13}C-labeled ubiquitin samples obtained in (red) PACC and (black) standard methods, together with (**e**) corresponding 1D slices at selected positions. The total experimental times were (red) 5.4 h and (black) 21.9 h in (d). All the experiments were performed at the spinning speed of 40 kHz with signal acquisitions under low-power TPPM decoupling at the RF fields of 7 kHz for 1.8 mg of ^{13}C-labeled ubiquitin. The data are modified from those in ref. 11.

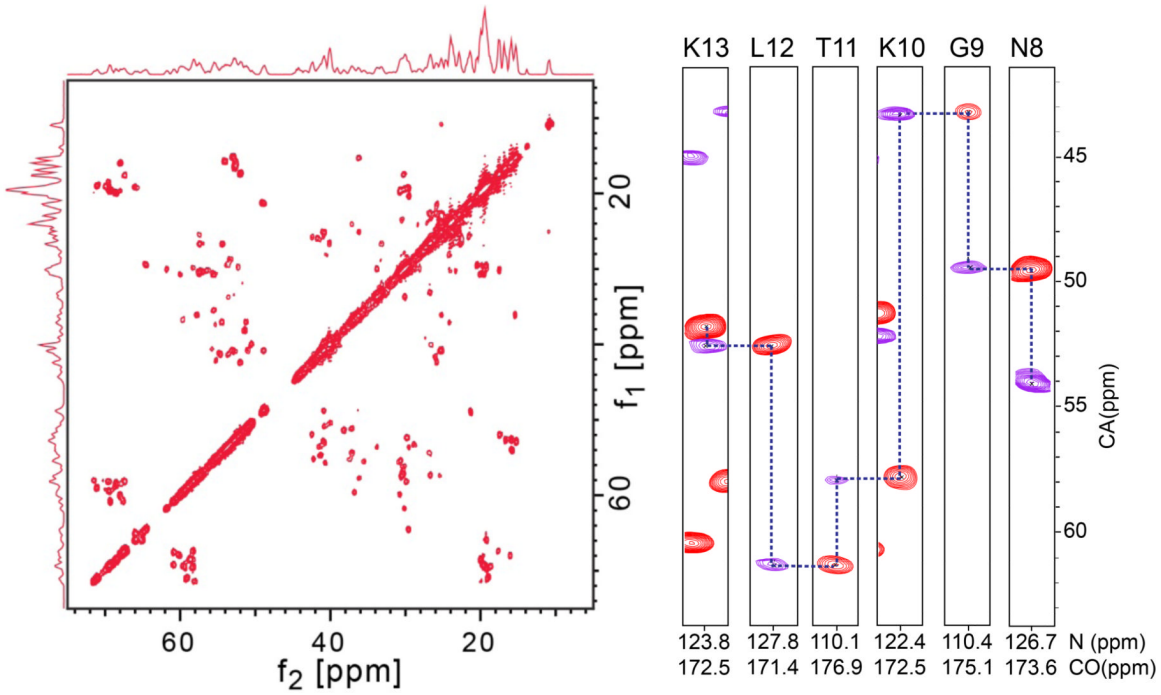

Figure 5.

(a) The aliphatic region of a 2D $^{13}C/^{13}C$ correlation SSNMR spectrum and (b) sequential assignments by 3D (purple) NCOCA and (red) CANCO spectra of GB1 micro-crystal sample incubated with 30 mM Cu^{2+}-EDTA. The data were collected at the ^{1}H frequency of 750 MHz using the PACC approach with a recycle delay of 300 ms using a Bruker 1.3 mm CPMAS triple-resonance probe. The experimental times were (a) 15 min and (b) 1 hour for each 3D data.

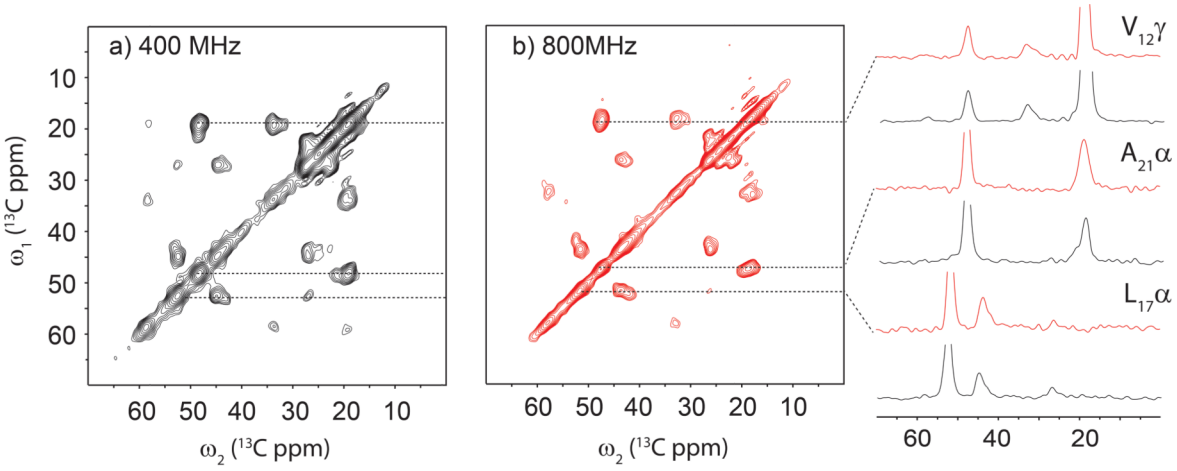

Figure 6.

A comparison of 2D $^{13}C/^{13}C$ correlation SSNMR spectra of Cu^{2+}-bound amyloid fibrils of Aβ(1-40) obtained at ^{1}H NMR frequencies of (a) 400 MHz with traditional scheme and at (b) 800 MHz with PACC scheme, together with (c) 1D slices. The total experimental times were (a) 32 h and (b) 1.9 h for (a) 2 mg and (b) 1 mg of the Aβ sample that was uniformly ^{13}C- and ^{15}N-labeled at selected residues Phe-4, Gly-9, Val-12, Leu-17, and Ala-21. The data in (a, b) were processed with Gaussian broadening of 1.0 ppm in both t_1 and t_2 periods. The data in (a) were acquired with the t_1 and t_2 periods of 4 ms and 8 ms, respectively on a Bruker Avance III 400 MHz spectrometer equipped with a homebuilt 2.5-mm CPMAS triple-resonance probe. For (a), a standard 2D $^{13}C/^{13}C$ correlation sequence was used under MAS at 20 kHz with high-power ^{1}H TPPM decoupling at the RF intensity of 90 kHz.[45] During the mixing period of 1.6 ms, the fpRFDR sequence[45] was applied with ^{13}C π-pulses of 15-μs width. The data in (b) was acquired in the PACC scheme with the t_1 and t_2 periods of 2 ms and 8 ms, respectively on a Bruker Avance 800 MHz spectrometer equipped with a JEOL 1-mm double-resonance CPMAS probe. In (b), ^{1}H lpTPPM decoupling was applied at 12.5 kHz in the t_1 and t_2 periods, and the fpRFDR mixing was applied during the mixing period of 1.92 ms with ^{13}C π-pulses of 7 μs widths.

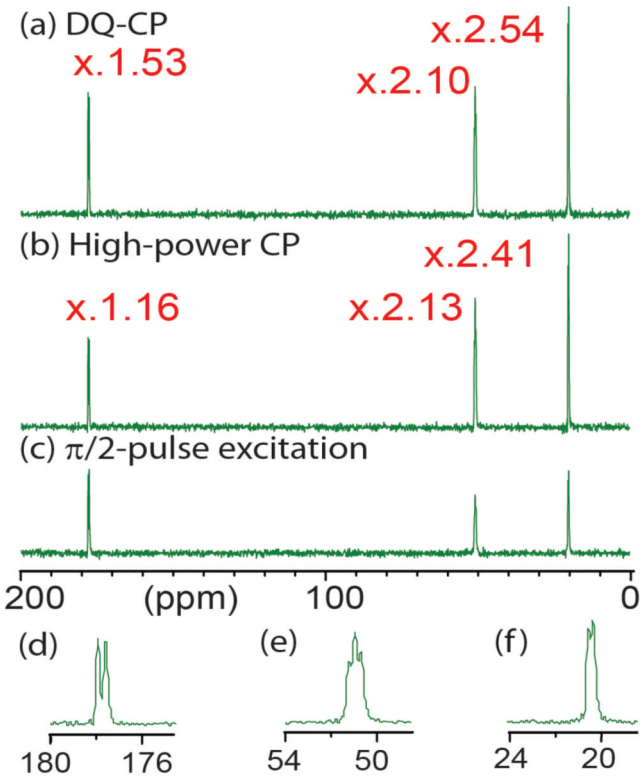

Figure 7.

(a, b) ^{13}C CPMAS SSNMR spectra of U ^{13}C, ^{15}N L-alanine under super fast MAS at $\omega_R/2\pi$ = 98 kHz. with (a) ramped DQ-CP ($\omega_H/2\pi$ ~74 kHz, $<\omega_C/2\pi>$ ~24 kHz) and (b) standard ramped CP ($\omega_H/2\pi$ ~250 kHz, $<\omega_C/2\pi>$ ~150 kHz) with a contact time of 2 ms compared to (c) a ^{13}C MAS spectrum by π/2-pulse excitation. The signals were collected with 4 scans with recycle delays of (a, b) 3 s and (c) 120 s, where ^{13}C T_1 ~ 40 s. The factors in (a, b) denote CP efficiencies, which are the signal intensities normalized by those in (c). (d-f) Magnified spectral regions of (a) for (d) CO_2^-, (e) CH, and (f) CH_3 groups. The data were collected with a JEOL 0.75-mm CPMAS double-resonance probe on a JEOL ECA 600 MHz spectrometer.